1/2(e^{2}/h) Conductance Plateau without 1D Chiral Majorana Fermions

Wenjie Ji and Xiao-Gang Wen

Phys. Rev. Lett. **120**, 107002 — Published 9 March 2018

DOI: 10.1103/PhysRevLett.120.107002

A mechanism of $\frac{1}{2}\frac{e^2}{h}$ conductance plateau without 1D chiral Majorana fermions

Wenjie Ji[1] and Xiao-Gang Wen[1]

[1] *Department of Physics, Massachusetts Institute of Technology, Cambridge, Massachusetts 02139, USA*

We address the question about the origin of the $\frac{1}{2}\frac{e^2}{h}$ conductance plateau observed in a recent experiment on an integer quantum Hall (IQH) film covered by a superconducting (SC) film. Since 1-dimensional (1D) chiral Majorana fermions on the edge of the above device can give rise to the half quantized plateau, such a plateau was regarded as a smoking-gun evidence for the chiral Majorana fermions. However, in this paper we give another mechanism for the $\frac{1}{2}\frac{e^2}{h}$ conductance plateau. We find the $\frac{1}{2}\frac{e^2}{h}$ conductance plateau to be a general feature of a good electric contact between the IQH film and SC film, and cannot distinguish the existence or the non-existence of 1D chiral Majorana fermions. We also find that the contact conductance between SC and an IQH edge channel has a non-Ohmic form $\sigma_{\text{SC-Hall}} \propto V^2$ in $k_BT \ll eV$ limit, if the SC and IQH bulks are fully gapped.

One promising direction in building a quantum computer is topological quantum computation [1], which can be realized using non-abelian topological orders that contain Ising non-abelian anyons, or other more general non-abelian anyons [2, 3]. Although Ising non-abelian anyons cannot perform universal topological quantum computation [4], they can be realized by non-interacting fermion systems, such as the vortex in $p+\mathrm{i}p$ 2D superconductor [5–7].

In 1993 [11], it was predicted that some non-abelian fractional quantum Hall states [2, 3] can have 1D chiral Majorana fermions on the edge. (1D chiral Majorana fermions are fermions with only fermion-number-parity conservation [8, 9] that propagate only in one direction in 1D space.) In fact, *the appearance of an odd number of 1D chiral Majorana fermion modes on the edge implies the appearance of non-abelian defects in the bulk [11, 12].* The non-abelian states may have already been realized in experiments [13–15]. In particular, the recently observed half quantized thermal Hall conductance [16] from the quantum Hall edge states [11, 17, 18] provides a smoking-gun evidence of 1D chiral Majorana fermions and its parent non-abelian fractional quantum Hall states. In 2000 [5], 1D chiral Majorana fermions were predicted to exist on the edge of $p+\mathrm{i}p$ 2D superconductor. More recently, 1D chiral Majorana fermions were predicted to exist on the interface of ferromagnet and superconductor on the surface of topological insulator [7], and on the edge of an IQH film covered by a SC film [19, 20].

In Ref. 19 and 20, it was shown that 1D chiral Majorana fermions can give rise to a $\frac{1}{2}\frac{e^2}{h}$ conductance plateau for a two terminal conductance σ_{12} across a Hall bar covered by a superconductor. Recently, Ref. 10 observed such a conductance plateau, which was regarded as a "distinct signature" of 1D chiral Majorana fermions. This leads to the claimed discovery of 1D chiral Majorana fermions. The discovered Majorana fermions were named "angel particles", and have attracted a lot of attention.

However, observing $\frac{1}{2}\frac{e^2}{h}$ conductance plateau may not imply the existence of 1D chiral Majorana fermions. For example, in Fig. 4A of the very same paper [10], $\frac{1}{2}\frac{e^2}{h}$ conductance was observed in a stacked IQH film and a metal film without the Majorana fermions. Similarly, Ref. 10 and 21 pointed out that $\frac{1}{2}\frac{e^2}{h}$ conductance can appear when the Hall bar under the SC film is in a metallic state without the Majorana fermions.

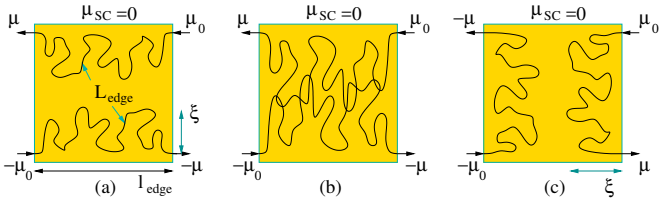

FIG. 1. A Hall bar covered by a SC film. The Hall bar under the superconductor can be in (a) a Chern number $N_{\text{Chern}} = 1$ IQH phase ($B > B_c$), (b) a metallic phase, and (c) a Chern number $N_{\text{Chern}} = 0$ insulating phase ($B < B_c$), depending on the correlation length ξ of the percolation model.

Such an explanation was discarded in Ref. 10 and 21 since it was thought to be inconsistent with the observed magnetic field B dependence of σ_{12} (Fig. 2C and Fig. 4A in Ref. 10). In the experiment, $\sigma_{12}(B)$ is found to be $\frac{1}{2}\frac{e^2}{h}$ at high field B where the topped film is normal metallic state. Then it increases up to $\frac{e^2}{h}$, as B is reduced and the topped film becomes SC. As B is reduced further, σ_{12} drops to a $\frac{1}{2}\frac{e^2}{h}$ plateau near B_c, and then to near 0.

Result: In this paper, we study the Majorana-fermionless mechanism for the $\frac{1}{2}\frac{e^2}{h}$ conductance plateau in detail. We find that it can explain the whole observed magnetic field B dependence of σ_{12} very well. The $\frac{1}{2}\frac{e^2}{h}$ conductance plateau can be a general feature of a good electric contact between the IQH and the SC films, regardless if the 1D chiral Majorana fermions exist or not.

A general understanding for two terminal conductance σ_{12}: In the experiment [10], the SC layer is directly deposited on the Hall bar. Naively, one would expect the contact resistance, $1/\sigma_{\text{SC-Hall}}$, between the superconductor and the edge channels of the Hall bar under the superconductor, to be much less than $\frac{h}{e^2} = 25812\Omega$. In this case, the two terminal conductance $\sigma_{12} = \frac{1}{2}\frac{e^2}{h}$. To

see this, we assume the superconductor to have a vanishing chemical potential $\mu_{SC} = 0$ and there is no net current flowing in or out of the superconductor. So the chemical potentials on the two incoming edge channels of the Hall bar should be opposite: μ_0 and $-\mu_0$. The chemical potentials on the two outgoing edge channels of the Hall bar are also opposite: μ and $-\mu$ (see Fig. 1).

When the contact resistance $1/\sigma_{\text{SC-Hall}}$ is low, the chemical potentials on the two outgoing edge channels vanish: $\mu = \mu_{SC} = 0$, and the two terminal conductance σ_{12} is given by $\sigma_{12} = \frac{\mu_0-(-\mu)}{\mu_0-(-\mu_0)} = \frac{1}{2}$. (In this paper, all conductances are measured in unit of $\frac{e^2}{h}$.) We see that the $\frac{1}{2}$ quantized conductance of σ_{12} is a very general feature of good contact between the superconductor and the Hall bar under the superconductor, and one might expect that the two terminal conductance σ_{12} to be always $\frac{1}{2}$. However, in the experiment, $\sigma_{12} \approx 1$ is observed for certain range of magnetic field. This suggests the other limit that the superconductor and the Hall bar decouples electronically, as then σ_{12} should be 1, contributed purely from the IQH bar. Indeed, that the contact resistance between the superconductor and the Hall bar can be much larger than $\frac{h}{e^2}$ is observed directly at corresponding fields via the measurement of σ_{13} shown in Fig.4C in Ref. 10.

The observed $\sigma_{12} = \frac{1}{2}$ at high field, where the topped film is metallic, indicates the contact resistance between the metal film and the Hall bar is always much less than $\frac{h}{e^2}$. But in the low field region where the film above IQH layer becomes SC, the measured σ_{12} varies from 1 to $\frac{1}{2}$ depending on B, indicating that the contact resistance $1/\sigma_{\text{SC-Hall}}$ between the SC film and the Hall bar can become much bigger than $\frac{h}{e^2}$, as well as much smaller. In this paper, we explain such a striking pattern of the contact conductance $\sigma_{\text{SC-Hall}}$ via a percolation model.

As the magnetic field B is reduced through the critical value B_c, the Hall bar under the superconductor changes from a Chern number $N_{\text{Chern}} = 1$ IQH state to a Chern number $N_{\text{Chern}} = 0$ insulating state. We use a percolation model to describe such a transition. In the percolation model, when B is reduced through B_c, the chiral edge channels of IQH state become more and more wiggled. Correspondingly, the Hall bar under the superconductor has three phases: the $N_{\text{Chern}} = 1$ phase in Fig. 1a and the $N_{\text{Chern}} = 0$ phase in Fig. 1c, where the IQH edge channel can be straight and short if B is far away from B_c. Thus the contact resistance $1/\sigma_{\text{SC-Hall}}$ is high. The third phase is a metallic phase in Fig. 1b, where the IQH edge channel fills the sample and its trajectory length L_{edge} is long. As a result, the contact resistance $1/\sigma_{\text{SC-Hall}}$ is low.

A microscopic calculation of the contact conductance $\sigma_{\text{SC-Hall}}$ between the superconductor and an IQH edge channel: We first assume the SC film and IQH bulk are clean enough that they are both fully gapped. Thus only Andreev scattering along the edge

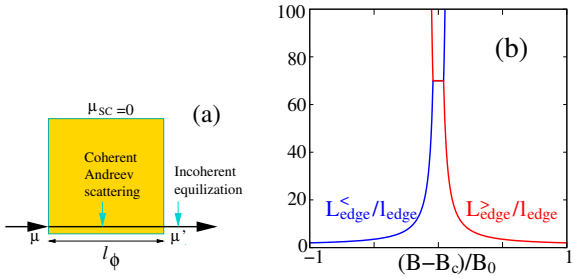

FIG. 2. (a) A segment of IQH edge under a superconductor. (b) $L^{>}_{\text{edge}}$ and $L^{<}_{\text{edge}}$ as a function of B.

contributes to $\sigma_{\text{SC-Hall}}$. To include the effects of charge conserving inelastic scattering, we first divide the IQH edge channel into many segments each of length l_ϕ – the dephasing length. Each segment is coupled to a superconductor (see Fig. 2a) which induces the coherent Andreev scattering: free electrons up to a chemical potential μ can be coherently scattered and come out as holes. The incoming edge state is an equilibrium state with an incoming chemical potential μ, while the outgoing edge state out of one SC segment is not an equilibrium state. Charge conserving inelastic scattering equilibrates the outgoing edge state, which now has an chemical potential μ'. From $\mu-\mu'$, we can determine $\sigma_{\text{SC-Hall}}$ for the segment.

To analyze the change in μ after passing a single SC segment, let us start with the equation of motion for free chiral fermion:

$$\mathrm{i}\hbar\dot{c} = v_f(-\mathrm{i}\partial_x - k_F)c + \frac{\mathrm{i}\hbar}{2}[v_{\text{sc}}\partial_x c^\dagger + \partial_x(v_{\text{sc}}c^\dagger)], \quad (1)$$

where v_f is the velocity of the chiral fermion, k_F is Fermi momentum at $\mu = E_F = 0$, and $v_{\text{sc}}(x)$ is the SC coupling coefficient which depends on x ($v_{\text{sc}} = 0$ for edge not under the superconductor). We treat $(c, c^\dagger) = (\psi_1, \psi_2) \equiv \psi^T$ as independent fields. For a mode with a frequency ω, the equation of motion becomes

$$\omega\psi = \begin{pmatrix} v_f(-\mathrm{i}\partial_x - k_F) & \frac{\mathrm{i}}{2}(v_{\text{sc}}\partial_x + \partial_x v_{\text{sc}}) \\ \frac{\mathrm{i}}{2}(v^*_{\text{sc}}\partial_x + \partial_x v^*_{\text{sc}}) & v_f(-\mathrm{i}\partial_x + k_F) \end{pmatrix}\psi \quad (2)$$

or (up to linear v_{sc} order)

$$-v_f \begin{pmatrix} 1 & \frac{v_{\text{sc}}}{2v_f} \\ \frac{v^*_{\text{sc}}}{2v_f} & 1 \end{pmatrix}^{-1} \mathrm{i}\partial_x \begin{pmatrix} 1 & \frac{v_{\text{sc}}}{2v_f} \\ \frac{v^*_{\text{sc}}}{2v_f} & 1 \end{pmatrix}^{-1} \psi$$
$$\approx \begin{pmatrix} \omega + v_f k_F & 0 \\ 0 & \omega - v_f k_F \end{pmatrix}\psi. \quad (3)$$

Let $\tilde{\psi} = \begin{pmatrix} 1 & \frac{v_{sc}}{2v_f} \\ \frac{v_{sc}^*}{2v_f} & 1 \end{pmatrix}^{-1} \psi$, we can rewrite the above as

$$
\begin{aligned}
-\mathrm{i}\partial_x \tilde{\psi}(x) &= M(x)\tilde{\psi}(x), \qquad (4)\\
M(x) &= \begin{pmatrix} 1 & \frac{v_{sc}}{2v_f} \\ \frac{v_{sc}^*}{2v_f} & 1 \end{pmatrix} \begin{pmatrix} \frac{\omega}{v_f} + k_F & 0 \\ 0 & \frac{\omega}{v_f} - k_F \end{pmatrix} \begin{pmatrix} 1 & \frac{v_{sc}}{2v_f} \\ \frac{v_{sc}^*}{2v_f} & 1 \end{pmatrix} \\
&\approx \frac{\omega}{v_f} \begin{pmatrix} 1 & \frac{v_{sc}(x)}{v_f} \\ \frac{v_{sc}^*(x)}{v_f} & 1 \end{pmatrix} + \begin{pmatrix} k_F & 0 \\ 0 & -k_F \end{pmatrix}.
\end{aligned}
$$

Solving the above differential equation, we find $\tilde{\psi}(x) = P[\mathrm{e}^{\mathrm{i}\int_0^x \mathrm{d}xM(x)}]\tilde{\psi}(0)$, where P is the path ordering. Now we assume that $v_{sc}(x) = 0$ for $x < 0$ and $x > l_\phi$, and $v_{sc}(x)$ is a constant for $x \in [0, l_\phi]$. We find $\psi(l_\phi) = S\psi(0)$, where the unitary matrix S is given by

$$
S = P[\mathrm{e}^{\mathrm{i}\int_0^{l_\phi} \mathrm{d}xM(x)}] = \mathrm{e}^{\mathrm{i}\phi} \begin{pmatrix} \mathrm{e}^{\mathrm{i}k_F l_\phi}\cos\theta & \mathrm{i}\,\mathrm{e}^{\mathrm{i}\varphi}\sin\theta \\ \mathrm{i}\,\mathrm{e}^{-\mathrm{i}\varphi}\sin\theta & \mathrm{e}^{-\mathrm{i}k_F l_\phi}\cos\theta \end{pmatrix}
$$

and, to the linear order in v_{sc}, the scattering angle is

$$
\theta \approx \frac{|v_{sc}|\omega}{k_F v_f^2}\sin(k_F l_\phi). \qquad (5)
$$

The modes with a frequency ω are electron-like state with momentum $k + k_F$ and hole-like state with momentum $-k + k_F$, where $k = \frac{\omega}{v_f}$. Denote a_k, b_k as incoming and outgoing electron annihilation operator of momentum k measured from k_F. b_k is determined by $b_k = S_{11}a_k + S_{12}a_{-k}^\dagger$.

In the zero temperature limit, the occupation numbers of incoming and outgoing electrons are $\langle a_k^\dagger a_k\rangle = 1$ for $k \le \frac{\mu}{\hbar v_f}$, $\langle a_k^\dagger a_k\rangle = 0$ for $k > \frac{\mu}{\hbar v_f}$, and

$$
\begin{aligned}
\langle b_k^\dagger b_k\rangle &= \cos^2\theta\langle a_k^\dagger a_k\rangle + \sin^2\theta\left(1 - \langle a_{-k}^\dagger a_{-k}\rangle\right) \\
&= \begin{cases} 0, & k > \frac{\mu}{\hbar v_f} \\ \cos^2(\theta(k)), & -\frac{\mu}{\hbar v_f} \le k \le \frac{\mu}{\hbar v_f} \\ 1, & k < -\frac{\mu}{\hbar v_f} \end{cases} \qquad (6)
\end{aligned}
$$

The outgoing electrons relax to μ' with the same density

$$
\int_{-\frac{\mu}{\hbar v_f}}^{\frac{\mu}{\hbar v_f}} \frac{dk}{2\pi}\cos^2\left(\frac{|v_{sc}|\sin(k_F l_\phi)}{v_f k_F}k\right) = \int_{-\frac{\mu}{\hbar v_f}}^{\frac{\mu'}{\hbar v_f}} \frac{dk}{2\pi} \qquad (7)
$$

$$
\Rightarrow \quad \mu' = \frac{\hbar v_f^2 k_F}{2|v_{sc}|\sin(k_F l_\phi)}\sin\frac{2|v_{sc}|\sin(k_F l_\phi)\mu}{\hbar v_f^2 k_F} \qquad (8)
$$

When $\frac{|v_{sc}|\mu}{\hbar v_f^2 k_F} \ll 1$, we have

$$
\mu' = \mu\left(1 - \frac{1}{6}\left(\frac{2|v_{sc}|\sin(k_F l_\phi)\mu}{\hbar v_f^2 k_F}\right)^2\right).
$$

This change of μ through one segment of length l_ϕ allows us to obtain, for a length δL_{edge} edge,

$$
\sigma_{\text{SC-Hall}} = -\frac{\delta\mu}{\mu} = \left(\frac{\mu}{\Delta}\right)^2\frac{\delta L_{\text{edge}}}{l_\phi} \qquad (9)
$$

with $\frac{1}{\Delta} = \sqrt{\frac{1}{3}}\frac{|v_{sc}|}{v_f^2\hbar k_F}$, where we have replaced $\sin^2(k_F l_\phi)$ by its average $\frac{1}{2}$. Interestingly, $\sigma_{\text{SC-Hall}}$ is proportional to μ^2, or rather, non-Ohmic.

In the high temperature limit,

$$
\begin{aligned}
\langle a_k^\dagger a_k\rangle &= g(\mu, k) \equiv \frac{1}{e^{\frac{\hbar v_f k - \mu}{k_B T}} + 1} \\
\langle b_k^\dagger b_k\rangle &= \cos^2\theta g(\mu, k) + \sin^2\theta(1 - g(\mu, -k)) \\
&= \cos^2\theta g(\mu, k) + \sin^2\theta g(-\mu, k).
\end{aligned} \qquad (10)
$$

Keep to the first order of $\frac{\mu}{k_B T}$ and $\frac{v_{sc}}{v_f}$, we reach

$$
\mu' = \mu\left[1 - \frac{2\pi^2}{3}\left(\frac{|v_{sc}|\sin(k_F l_\phi)}{v_f k_F}\frac{k_B T}{\hbar v_f}\right)^2\right]. \qquad (11)
$$

From this we obtain, for a length δL_{edge} edge,

$$
\sigma_{\text{SC-Hall}} = \gamma\frac{\delta L_{\text{edge}}}{l_\phi}. \qquad (12)
$$

with $\gamma = \frac{\pi^2}{3}\left(\frac{|v_{sc}|k_B T}{\hbar v_f^2 k_F}\right)^2$. In this case, $\sigma_{\text{SC-Hall}}$ is independent of μ and is Ohmic.

If either the SC film or IQH bulk are not clean enough and have gapless electronic states that couple to the chiral edge channel, we can take into account those gapless states by assuming the superconductor to be a gapless superconductor. In this case, $\sigma_{\text{SC-Hall}}$ will in addition receive a contribution from the electron tunneling into the quasiparticle states in the gapless superconductor. We expect such a contribution to be Ohmic and $\sigma_{\text{SC-Hall}}$ can be modeled by (12) in all temperature range.

In the following, we will separately calculate $\sigma_{12}(B)$, using the non-Ohmic (9) or Ohmic (12) $\sigma_{\text{SC-Hall}}$.

Non-Ohmic case: From (9), we see that the contact resistance can be much bigger than $\frac{h}{e^2}$, as long as $\mu^2\delta L_{\text{edge}}$ is small enough. The current $\delta I = \sigma_{\text{SC-Hall}}\ \mu$ flowing from the edge to the superconductor will cause a drop in the chemical potential μ along the edge:

$$
\mathrm{d}\mu(x) = -\sigma_{\text{SC-Hall}}\ \mu = -\frac{\mu^3(x)}{l_\phi\Delta^2}\mathrm{d}x \qquad (13)
$$

Solving the above equation, we find $\mu = \mu(L_{\text{edge}}) = \mu_0/\sqrt{\frac{2\mu_0^2}{\Delta^2 l_\phi}L_{\text{edge}} + 1}$ for an edge of length L_{edge}.

Therefore, for $B > B_c$ (see Fig. 1a)

$$
\sigma_{12} = \frac{\mu_0 + \mu}{2\mu_0} = \frac{\mu_0 + \frac{\mu_0}{\sqrt{\frac{2\mu_0^2}{\Delta^2 l_\phi}L_{\text{edge}}^> + 1}}}{2\mu_0}, \qquad (14)
$$

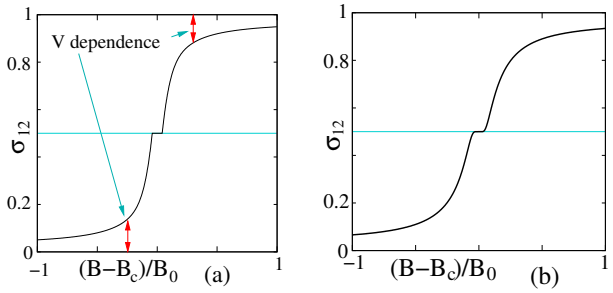

FIG. 3. Two terminal conductance σ_{12} as a function of magnetic field B. (a) Non-Ohmic case (18), with $l_{\rm edge}/a = 70$ and $\frac{2\mu_0^2 l_{\rm edge}}{\Delta^2 l_\phi} = 0.12$. Deviation of σ_{12} from $\frac{e^2}{h}$ and 0 will have a clear voltage $V = \mu_0/e$ dependence. (b) Ohmic case (19), with $\gamma\frac{l_{\rm edge}}{l_\phi} = 1/14$. The curve for Ohmic case is independent of the percolation cut-off length scale a.

In a percolation cluster of size ξ, the edge length is $\frac{\xi^2}{a}$, where a is the cut-off length scale of the percolation model. The total edge length is $L^>_{\rm edge} = \frac{l_{\rm edge}}{\xi}\frac{\xi^2}{a} = l_{\rm edge}\frac{\xi}{a}$. The linear size of the percolation cluster ξ scales as

$$\xi = a\Big(\frac{|B_c - B|}{B_0}\Big)^{-\nu} + a, \quad \nu = 1.33 \tag{15}$$

With the above choice, we see that $(L^>_{\rm edge}, \sigma_{12}) \to (l_{\rm edge}, 1)$ as $B \to \infty$ (assuming $\frac{2l_\phi\mu_0^2}{\hbar^2 v_f^2} l_{\rm edge}$ is small), and $(L^>_{\rm edge}, \sigma_{12}) \to (\infty, \frac{1}{2})$ as $B \to B_c$.

But ξ can only increase up to $l_{\rm edge}$, the width of superconductor covered Hall bar, beyond which ξ remains to be $l_{\rm edge}$ in the metallic phase in Fig. 1b . To model such a behavior, we choose

$$\begin{aligned} L^>_{\rm edge} &= a^{-1}\xi l_{\rm edge}\Theta(B - B_c)\Theta(l_{\rm edge} - \xi) \\ &+ a^{-1}l_{\rm edge}^2\Theta(\xi - l_{\rm edge}) \\ &+ a^{-1}l_{\rm edge}^2 \mathrm{e}^{(l_{\rm edge}-\xi)/\xi}\Theta(B_c - B)\Theta(l_{\rm edge} - \xi). \end{aligned} \tag{16}$$

where $\Theta(x) = 1$ if $x > 0$ and $\Theta(x) = 0$ if $x < 0$. When $B > B_c$, the above gives $L^>_{\rm edge} = a^{-1}\xi l_{\rm edge}$ or $a^{-1}l^2_{\rm edge}$ near B_c (see Fig. 2b). When B is much less than B_c, we also assign $L^>_{\rm edge}$ a very large value to make $\mu_0/\sqrt{\frac{2\mu_0^2}{\Delta^2 l_\phi}L^>_{\rm edge} + 1}$ vanishes. This allows us to combine the $B > B_c$ and $B < B_c$ results together later. For $B < B_c$ (see Fig. 1c)

$$\begin{aligned} \sigma_{12} &= \frac{\mu_0 - \mu}{2\mu_0} = \frac{\mu_0 - \frac{\mu_0}{\sqrt{\frac{2\mu_0^2}{\Delta^2 l_\phi}L^<_{\rm edge}+1}}}{2\mu_0}, \\ L^<_{\rm edge} &= a^{-1}\xi l_{\rm edge}\Theta(B_c - B)\Theta(l_{\rm edge} - \xi) \\ &+ a^{-1}l_{\rm edge}^2\Theta(\xi - l_{\rm edge}) \\ &+ a^{-1}l_{\rm edge}^2 \mathrm{e}^{(l_{\rm edge}-\xi)/\xi}\Theta(B - B_c)\Theta(l_{\rm edge} - \xi) \end{aligned} \tag{17}$$

We can combine the $B > B_c$ and $B < B_c$ cases:

$$\sigma_{12} = \frac{1}{2}\left(1 + \frac{1}{\sqrt{\frac{2\mu_0^2}{\Delta^2 l_\phi}L^>_{\rm edge} + 1}} - \frac{1}{\sqrt{\frac{2\mu_0^2}{\Delta^2 l_\phi}L^<_{\rm edge} + 1}}\right) \tag{18}$$

With the above design of $L^>_{\rm edge}$ and $L^<_{\rm edge}$, only one of the two terms in $\frac{1}{\sqrt{\frac{2\mu_0^2}{\Delta^2 l_\phi}L^>_{\rm edge}+1}} - \frac{1}{\sqrt{\frac{2\mu_0^2}{\Delta^2 l_\phi}L^<_{\rm edge}+1}}$ contributes in either the $N_{\rm Chern} = 1$ phase or the $N_{\rm Chern} = 0$ phase. In the metallic phase (see Fig. 1b), both terms are small, and their difference makes the contribution even smaller. This gives rise to $\frac{1}{2}$ quantized two terminal conductance. The above result is plotted in Fig. 3a. Such a result is very close to what was observed in Ref. 10. But it has a very different mechanism than what was proposed in Ref. 19 and 20. In our non-Ohmic case, the $\sigma_{12} = \frac{1}{2}\frac{e^2}{h}$ plateau roughly corresponds to the metallic phase in Fig. 1 where $\xi/l_{\rm edge} \approx 1$, with no need to introduce 1D chiral Majorana fermion on the edge.

Ohmic case: From (12), we see that the contact resistance can be much bigger than $\frac{h}{e^2}$, if $\gamma\delta L_{\rm edge}/l_\phi$ is small enough. From the equation $\mathrm{d}\mu(x) = -\gamma\frac{\mathrm{d}x}{l_\phi}\mu(x)$ and for a given total length of the edge channel $L_{\rm edge}$, we find $\mu = \mu_0\,\mathrm{e}^{-\gamma L_{\rm edge}/l_\phi}$. Therefore, for $B > B_c$ (see Fig. 1a) $\sigma_{12} = \frac{\mu_0+\mu}{2\mu_0} = \frac{1+\mathrm{e}^{-\gamma L_{\rm edge}/l_\phi}}{2}$, where $L_{\rm edge} = \frac{l_{\rm edge}}{\xi}\frac{\xi^2}{a} = l_{\rm edge}\frac{\xi}{a}$. With ξ given in (15), we see that $L_{\rm edge} \to l_{\rm edge}$ as $B \to \infty$ and $L_{\rm edge} \to \infty$ as $B \to B_c$. Similarly, for $B < B_c$ (see Fig. 1c), $\sigma_{12} = \frac{\mu_0-\mu}{2\mu_0} = \frac{1-\mathrm{e}^{-\gamma L_{\rm edge}/l_\phi}}{2}$. We can combine the $B > B_c$ and $B < B_c$ cases together:

$$\sigma_{12} = \frac{1 + \mathrm{sgn}(B - B_c)\,\mathrm{e}^{-(\frac{B_0^\nu}{|B_c - B|^\nu}+1)\frac{\gamma l_{\rm edge}}{l_\phi}}}{2}. \tag{19}$$

The above result is plotted in Fig. 3b. Such a result for Ohmic case is also very close to what was observed in Ref. 10. But for Ohmic case, the $\sigma_{12} = \frac{1}{2}\frac{e^2}{h}$ plateau is much broader than the metallic phase in Fig. 1.

Summary: In the percolation model, we considered two possible cases, Ohmic case and non-Ohmic case, both can explain the $\sigma_{12}(B)$ cuve in the experiment Ref. 10. More experiments are needed to see which case applies. If an Ohmic contact conductance is observed, it will indicate either the SC and/or IQH bulks have gapless electronic states, or the electron temperature is high.

If a non-Ohmic contact conductance $\sigma_{\text{SC-Hall}}$ between the superconductor and the IQH edge channel is observed near $\sigma_{12} \sim 0$ or $\sigma_{12} \sim 1$, it will indicate the SC and IQH bulks to be fully gapped. Therefore observing a non-Ohmic contact conductance is a sign of clean samples, which is necessary for further strong quantum coherent phenomena. For instance, on such samples at low enough temperature, the dephasing length can become large, and 1D chiral Majorana fermions can appear.

After posting this paper, another paper Ref. 22 was posted where the same conclusion was reached via a similar consideration. A month later, Ref. 23 was posted, where the dephasing length l_ϕ is assumed to be larger than the "$p+\mathrm{i}p$ SC coherence length" $\xi_{p+\mathrm{i}p}$ (put it another way, the minimum width of a $p+\mathrm{i}p$ SC stripe such that 1D chiral Majorana fermions on the two edges are well separated). In this case, the 1D chiral Majorana edge mode can be well defined, and give rise to a $\frac{1}{2}\frac{e^2}{h}$ plateau in σ_{12}. In this paper, we consider the opposite limit $l_\phi < \xi_{p+\mathrm{i}p}$ without coherent 1D chiral Majorana edge mode, and show that there is still a $\frac{1}{2}\frac{e^2}{h}$ plateau. Furthermore, the B dependence of σ_{12} can agree with the experiment very well, with a proper choice of some parameters. In particular, if we choose $B_0 \sim 200$mT, the plateau width will be about 20mT (see Fig. 3).

We would like to thank K. L. Wang, Yayu Wang, and Shoucheng Zhang for very helpful discussions. This research was supported by NSF Grant No. DMR-1506475 and NSFC 11274192.

[1] A. Y. Kitaev, Ann. Phys. (N.Y.) **303**, 2 (2003).
[2] X.-G. Wen, Phys. Rev. Lett. **66**, 802 (1991).
[3] G. Moore and N. Read, Nucl. Phys. B **360**, 362 (1991).
[4] M. Freedman, M. Larsen, and Z. Wang, Commun. Math. Phys. **227**, 605 (2002).
[5] N. Read and D. Green, Phys. Rev. B **61**, 10267 (2000).
[6] D. A. Ivanov, Phys. Rev. Lett. **86**, 268 (2001), cond-mat/0005069.
[7] L. Fu and C. L. Kane, Physical Review Letters **100**, 096407 (2008), arXiv:0707.1692.
[8] X.-L. Qi, C. Xu, and X.-G. Wen, Quantum particles: Dirac, Weyl, and Majorana, http://chuansong.me/n/1063337646169 (2016).
[9] X.-G. Wen, to apeear in RMP (2016), arXiv:1610.03911.
[10] Q. L. He, L. Pan, A. L. Stern, E. C. Burks, X. Che, G. Yin, J. Wang, B. Lian, Q. Zhou, E. S. Choi, K. Murata, X. Kou, Z. Chen, T. Nie, Q. Shao, Y. Fan, S.-C. Zhang, K. Liu, J. Xia, and K. L. Wang, Science **357**, 294 (2017), arXiv:1606.05712.
[11] X.-G. Wen, Phys. Rev. Lett. **70**, 355 (1993).
[12] X.-G. Wen and A. Zee, Phys. Rev. B **46**, 2290 (1992).
[13] R. Willett, J. P. Eisenstein, H. L. Strörmer, D. C. Tsui, A. C. Gossard, and J. H. English, Phys. Rev. Lett. **59**, 1776 (1987).
[14] M. Dolev, M. Heiblum, V. Umansky, A. Stern, and D. Mahalu, Nature (London) **452**, 829 (2008), arXiv:0802.0930.
[15] I. P. Radu, J. B. Miller, C. M. Marcus, M. A. Kastner, L. N. Pfeiffer, and K. W. West, Science **320**, 899 (2008), arXiv:0803.3530.
[16] M. Banerjee, M. Heiblum, V. Umansky, D. E. Feldman, Y. Oreg, and A. Stern, (2017), arXiv:1710.00492.
[17] X.-G. Wen, Phys. Rev. B **41**, 12838 (1990).
[18] C. L. Kane and M. P. A. Fisher, Phys. Rev. B **55**, 15832 (1997), cond-mat/9603118.
[19] S. B. Chung, X.-L. Qi, J. Maciejko, and S.-C. Zhang, Phys. Rev. B **83**, 100512 (2011), arXiv:1008.2003.
[20] J. Wang, Q. Zhou, B. Lian, and S.-C. Zhang, Phys. Rev. B **92**, 064520 (2015), arXiv:1507.00788.
[21] C.-Z. Chen, J. J. He, D.-H. Xu, and K. T. Law, Phys. Rev. B **96**, 041118 (2017), arXiv:1608.00237.
[22] Y. Huang, F. Setiawan, and J. D. Sau, (2017), arXiv:1708.06752.
[23] B. Lian, J. Wang, X.-Q. Sun, A. Vaezi, and S.-C. Zhang, (2017), arXiv:1709.05558.